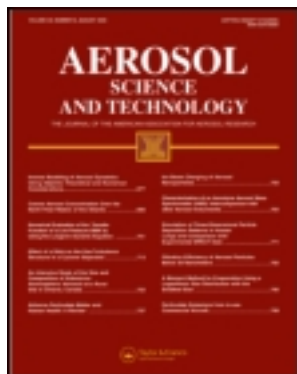


This article was downloaded by: [US EPA Library]

On: 08 September 2011, At: 09:28

Publisher: Taylor & Francis

Informa Ltd Registered in England and Wales Registered Number: 1072954 Registered office: Mortimer House, 37-41 Mortimer Street, London W1T 3JH, UK



Aerosol Science and Technology

Publication details, including instructions for authors and subscription information:

<http://www.tandfonline.com/loi/uast20>

Differences in the OC/EC Ratios that Characterize Ambient and Source Aerosols due to Thermal-Optical Analysis

Bernine Khan^a, Michael D. Hays^a, Chris Geron^a & James Jetter^a

^a Office of Research and Development, National Risk Management Research Laboratory, US Environmental Protection Agency, Research Triangle Park, North Carolina, USA

Available online: 03 Aug 2011

To cite this article: Bernine Khan, Michael D. Hays, Chris Geron & James Jetter (2012): Differences in the OC/EC Ratios that Characterize Ambient and Source Aerosols due to Thermal-Optical Analysis, *Aerosol Science and Technology*, 46:2, 127-137

To link to this article: <http://dx.doi.org/10.1080/02786826.2011.609194>

PLEASE SCROLL DOWN FOR ARTICLE

Full terms and conditions of use: <http://www.tandfonline.com/page/terms-and-conditions>

This article may be used for research, teaching and private study purposes. Any substantial or systematic reproduction, re-distribution, re-selling, loan, sub-licensing, systematic supply or distribution in any form to anyone is expressly forbidden.

The publisher does not give any warranty express or implied or make any representation that the contents will be complete or accurate or up to date. The accuracy of any instructions, formulae and drug doses should be independently verified with primary sources. The publisher shall not be liable for any loss, actions, claims, proceedings, demand or costs or damages whatsoever or howsoever caused arising directly or indirectly in connection with or arising out of the use of this material.



Differences in the OC/EC Ratios that Characterize Ambient and Source Aerosols due to Thermal-Optical Analysis

Bernine Khan, Michael D. Hays, Chris Geron, and James Jetter

Office of Research and Development, National Risk Management Research Laboratory,
US Environmental Protection Agency, Research Triangle Park, North Carolina, USA

Different thermal-optical methods used to measure OC/EC and EC/TC ratios in atmospheric aerosols often produce significantly different results due to variations within the temperature programming and optical techniques of each method. To quantify the thermal and optical effects on these ratios, various source (residential cookstoves and diesel exhaust) and atmospheric (rural and urban) aerosols were analyzed using 3 thermal protocols: (1) two modified versions of the Birch and Cary (1996, Elemental Carbon-Based Method for Monitoring Occupational Exposures to Particulate Diesel Exhaust. *Aerosol Sci. Technol.*, 25:221–241) National Institute of Occupational Safety and Health (NIOSH 5040) protocol—designated in this paper as NIOSH and NIST-EPA protocols, and (2) the IMPROVE (the Interagency Monitoring of Protected Visual Environments) protocol outlined by Chow et al. 1993 (The DRI Thermal/Optical Reflectance Carbon Analysis System: Description, Evaluation, and Applications in U.S. Air Quality Studies. *Atmos. Environ.*, 27:1185–1201)—designated in this paper as IMPROVE protocol. The use of a dual-optical instrument permitted simultaneous monitoring of the transmission (TOT [thermal-optical transmission]) and reflectance (TOR [thermal-optical reflectance]) for each protocol. Results show that the aerosols containing components susceptible to charring (such as water-soluble organic compounds typical of cookstove and rural aerosols) had higher OC/EC variability among the methods when compared with diesel-impacted aerosols (diesel and urban), which showed little to no “instrumentally calculated” pyrolyzed carbon (PyC). Thermal effects on the OC/EC ratios among the 3 TOT methods were significantly lower for diesel-impacted aerosols. Similar OC/EC findings were observed for the 3 TOR methods. Optical effects (TOT/TOR ratio) for the OC/EC ratio ranged from 1.37–1.71 (residential cookstoves), 1.63–2.23 (rural), 1.05–1.24 (diesel exhaust), and 0.80–1.12 (urban) for the 3 methods, with IMPROVE (TOT and TOR) always significantly lower when compared with NIST-EPA (TOT

and TOR) and NIOSH (TOT and TOR) for all sample types. Thermal and optical effects on the EC/TC ratios were similar to those observed for the OC/EC ratios. Due to their distinct aerosol characteristics, different sample types behave differently under various thermal and optical conditions. Hence, use of a single TOA method to define OC/EC ratios for all aerosol types may not be feasible.

[Supplementary materials are available for this article. Go to the publisher’s online edition of *Aerosol Science and Technology* to view the free supplementary files.]

INTRODUCTION

Fine particle matter (PM_{2.5}) in the atmosphere is linked to human health effects (Kagawa 2002; Pope and Dockery 2006), reduces visibility (Watson 2002), and alters the earth’s radiative balance by scattering and absorbing incoming solar radiation (IPCC 2007). Atmospheric fine aerosols consist of a carbonaceous fraction frequently chemically defined as organic carbon (OC) and elemental carbon (EC) using thermal-optical analysis (TOA). Long-term atmospheric monitoring and source emissions testing has produced TOA-based OC/EC data used in air quality, dispersion, and climate models that forecast regional and global weather patterns (Hansen et al. 2000; Jacobson 2001). TOA involves collecting aerosol deposits on quartz-fiber filters and subjecting a filter punch to a 2-phased heating process, first in an oxygen-free, helium environment (He) and then through a 2% O₂ environment (He-Ox) (Figure 1). Ideally, volatile and semivolatile OC evolves by thermal desorption in the He phase, and EC evolves following oxidation in the He-Ox phase of the analysis. Carbon evolved at each phase passes over a catalyst bed where it is oxidized to CO₂, then converted to CH₄ and detected by a flame ionization detector (FID). A major drawback of this analysis is that during the He phase, certain carbon compounds (presumably OC) pyrolyze or “char” to form an EC-like material. Both the charred OC and native EC oxidize simultaneously either during the He phase or He-Ox phase of analysis. Charred OC and native EC are assumed to possess similar chemical and optical properties and hence are differentiated by continuously monitoring the formation and evolution of

Received 23 November 2010; accepted 23 June 2011.

The authors would like to thank Dr. Seung Cho from the U.S. EPA in RTP North Carolina for providing diesel samples and Dr. Michael Gatari from the University of Nairobi in Kenya for providing the urban ambient samples.

Address Correspondence to Michael D. Hays, Office of Research and Development, National Risk Management Research Laboratory, U.S. Environmental Protection Agency, 109 TW Alexander Dr, Research Triangle Park, NC 27711, USA. E-mail: hays.michael@epa.gov

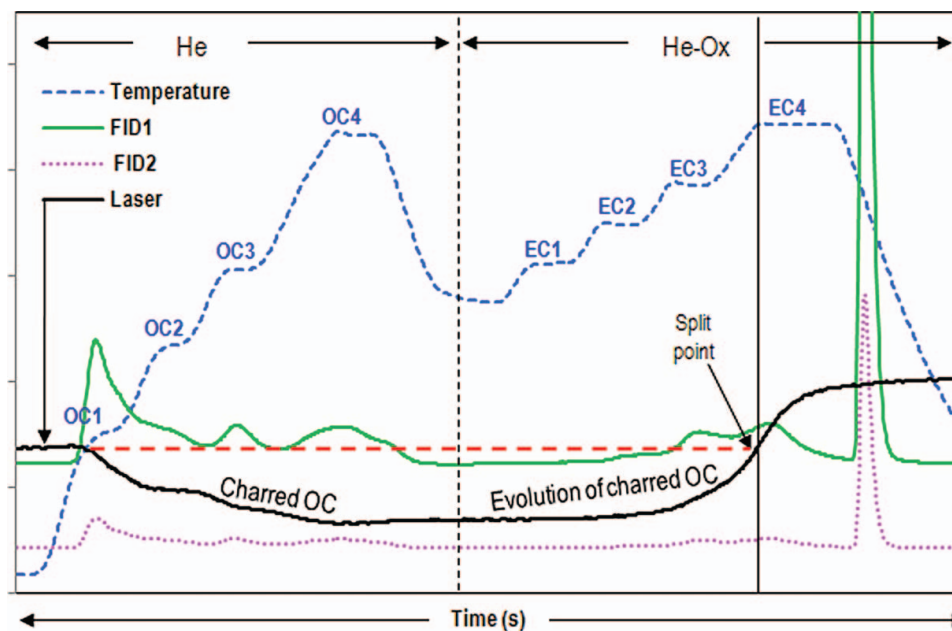


FIG. 1. Typical NIOSH TOT thermogram. The split point is determined from the laser absorbance in the He-Ox phase to the initial absorbance in the He phase (designated as horizontal dashed line). Char production is defined by attenuation of the laser signal and char evolution defined by the increase in the laser signal prior to EC evolution. FID1 (solid line)—carbon species at 100% signal, FID2 (dotted line)—carbon species at 25% signal, laser transmission (solid line), and temperature protocol (dashed line) (color figure available online).

charred OC throughout the filter media via transmittance (TOT) or reflectance (TOR) using an optical laser ($\lambda = 680 \text{ nm}$). Without this optical correction, charred OC will be measured as EC, thus rendering higher EC values. The “automated” OC/EC split with optical correction by TOA is based on the assumptions that (1) char originates from OC only and (2) all char evolves prior to EC evolution.

The National Institute of Occupational Safety and Health (NIOSH) thermal-optical transmission (TOT) (Birch and Cary 1996) and the IMPROVE (Interagency Monitoring of Protected Visual Environments) thermal-optical reflectance (TOR) (Chow et al. 1993) methods are 2 widely applied TOA methods. For a given sample, both methods agree on the total carbon (TC) (i.e., summation of OC and EC) but can significantly disagree on the OC/EC ratio (Countess 1990; Chow et al. 2001; Schauer et al. 2003). Variability of the OC/EC ratio among the methods has been attributed to the different temperature protocols, specifically the maximum temperature in the He phase (He-T_{max}) (Zhi et al. 2009) and the optical technique used for charring correction (Chow et al. 2001). Some studies argue that He-T_{max} in the NIOSH Method (870°C) is too high and promotes charring or too low in the IMPROVE method (550°C) so that OC is not sufficiently removed (Subramanian et al. 2006). The residence times at each temperature step within the He and He-Ox phases are fixed for NIOSH but vary for IMPROVE depending on the sample composition. Hence, a sample individually subjected to both methods will encounter a wide range of temperature ramp rates that can alter sample chemistry and consequently influence

char formation during the analysis. OC/EC discrepancies have also been linked to the presence of organic vapors within the body of the filter (a positive artifact during sample collection). Particulate OC on the surface of the filter, as well as, organic vapors within the body of the filter both char during TOA. Since during transmittance (TOT), the laser penetrates the filter media and during reflectance (TOR), the laser records only the surface of the filter, charring occurring within the body of the filter is not recorded when using TOR. OC values under TOT methods can therefore be higher than TOR methods since the char within the filter body during TOR is not recorded back to the OC concentration. To remove organic vapors and reactive substances during sample collection, a denuder or a back up quartz filter is utilized (Mader et al. 2001; Subramanian et al. 2004).

Some studies using ambient samples modify the temperature protocol of the NIOSH TOT method to minimize charring and other positive artifacts that bias OC/EC ratios (Schmid et al. 2001; Subramanian et al. 2006; Cavalli et al. 2010). One study, however, presents a temperature protocol for high- and low-charring aerosols by optically optimizing the NIOSH TOT method by altering (1) the He-T_{max} and its corresponding residence time and (2) the heating protocol of the He-Ox phase, to determine the point at which the mass absorption cross-section for charring is equivalent to native EC ($\sigma_{char} = \sigma_{EC}$) (i.e., where Beer’s Law is satisfied) (Conny 2007). The mass absorption cross-section (σ) is a measure of the absorbance of a material at a particular wavelength (λ) per unit area and concentration expressed in units of m^2/g . Many of the modified NIOSH

TOT methods, including the Conny (2007) protocol, were established using atmospheric aerosols obtained from multiple U.S. locations but have not been extensively evaluated using source-dominated aerosols.

This study quantifies the thermal and optical effects on the carbon ratios (OC/EC and EC/TC) obtained from 3 protocols—(1) the Conny (2007) protocol (referred to in this paper as the NIST-EPA protocol), (2) an upward adjustment of the Birch and Cary (1996) NIOSH protocol (referred to in this paper as the NIOSH protocol), which is comparable to what other studies, including the Ace-Asia study, have used when operating the Sunset Laboratory Instrument (Yang and Yu 2002; Yu et al. (2002); Schauer et al. (2003)), and (3) the IMPROVE protocol as outlined by Chow et al. 1993 (referred to in this paper as the IMPROVE protocol). The 3 protocols were tested on a variety of source sample types, including biomass burning aerosols emitted from residential cookstoves and diesel-generated exhaust. These sources are substantial contributors to the global EC inventory (Bond et al. 2004) and residential cookstoves, in particular, are central to atmospheric brown cloud (ABC) formation and thus widely modeled (USAID 2010). ABCs are layers of air pollution consisting of aerosols that contain black carbon (BC), OC, and dust that absorb and scatter solar radiation (Crutzen and Ramanathan 2003). ABCs should not be confused with brown carbon which is light-absorbing organic carbon. Few studies investigate the extent to which thermal-optical protocols may vary the EC/TC and OC/EC ratios in aerosols emitted from the wide range of cookstoves and fuels currently in use today. Other samples types included in the present study include atmospheric aerosol samples from a rural U.S. forest and an urban African location likely impacted by diesel and biomass sources. All TOA experiments were carried out on a single dual-optical carbon analyzer (Sunset Laboratory Dual Optics) that monitored charring by simultaneously measuring filter transmission and reflectance. Use of a single carbon analyzer minimizes analytical uncertainties typically produced when using different instruments to conduct NIOSH and IMPROVE protocols and to improve the quantification of OC/EC and EC/TC differences among TOA protocols. By using a dual-optical analyzer, the optical effects on these carbon ratios could be examined for the different protocols (i.e., NIST-EPA TOT and TOR, NIOSH TOT and TOR, and IMPROVE TOT and TOR) within each individual sample type. *Caution is advised in trying to make comparisons between Sunset IMPROVE TOR data obtained in this study and IMPROVE TOR data obtained by the Desert Research Institute (DRI) IMPROVE system since instrumentation differences may exist.* This study examines *only* the differences in temperature programming and optical reflectance/transmittance and not the differences due to instrumentation.

EXPERIMENTAL APPROACH

Thermal-Optical Methods

For this study, the 3 thermal-optical protocols (NIST-EPA, NIOSH, and IMPROVE) were executed on a single thermal-

optical carbon analyzer to reduce instrumental bias. The carbon analyzer used was the Sunset Laboratory Dual Optics (transmission and reflectance) Carbon Analyzer. Figure 1 shows a typical thermogram for the NIOSH transmission method. The temperature protocols for NIST-EPA, NIOSH, and IMPROVE are outlined in Table 1. TOA analysis involves 2 simultaneous analyses: (1) thermal evolution of OC during the He phase and EC during the He-Ox phase (or sometimes also in the He phase) using a specified temperature protocol (dashed line in Figure 1) and (2) optical measurement of the formation and evolution of char via laser absorbance (solid line in Figure 1). The depression of the laser signal indicates how much char is formed. As the laser signal increases, char and EC evolve. Since there is no distinction between the charred OC and EC, the instrument calculates how much OC has charred from the time the laser increases to the point where the laser matches the initial absorbance measured when the sample was first introduced into the oven (horizontal dashed line). At this point, the “automated” OC/EC split point is determined. Note that when using this instrument, the output file designates the evolution of char with a negative sign ($-PyC$) if it evolves in the He phase and positive sign ($+PyC$) if it evolves in the He-Ox phase. Summation of $-PyC$ and $+PyC$ indicates how much charred or pyrolyzed OC is added back to OC ($+PyC$) or subtracted from OC ($-PyC$). Throughout this manuscript, PyC is defined as the “instrumentally-calculated” PyC . Carbon measured before the split point is designated as OC, and carbon after the split is considered EC.

The dual-optics instrument utilized for this study was previously installed and characterized at NIST Gaithersburg, MD as described by Conny (2007). It was equipped with sophisticated PID (proportional-integral-differential) temperature control. Prior to initiating the study at EPA, the instrument manufacturer confirmed the accuracy of the oven temperature readings and laser alignment and laser power output. The mass flow controllers used to control gas deliveries were calibrated using a Gilibrator[®] system. Instrument blanks and sucrose standards were analyzed daily. The average instrument blank was $0.02 \pm 0.03 \mu\text{g-TC}/\text{cm}^2$ (for all methods) and sucrose recoveries within $\pm 3\%$ of a known concentration (for all methods). Daily instrument blanks and sucrose standards were analyzed using a different method (NIST-EPA, NIOSH, or IMPROVE) selected at random. Instrumental range for OC was between $7.25\text{--}600 \mu\text{g}/\text{cm}^2$ and for EC was $1.45\text{--}25 \mu\text{g}/\text{cm}^2$. All samples were collected on a pre-fired (550°C , 12 h) Pall Gelman quartz fiber filter.

Sample Information

A total of 171 aerosol samples, consisting of varying amounts of OC and EC fractions, from a variety of ambient and source-dominated emissions were selected for this study. Total carbon loading for the different sample types ranged from $3\text{--}113 \mu\text{g}/\text{cm}^2$ (residential cookstove), $9\text{--}45 \mu\text{g}/\text{cm}^2$ (diesel), $2\text{--}37 \mu\text{g}/\text{cm}^2$ (rural ambient), and $32\text{--}175 \mu\text{g}/\text{cm}^2$ (urban ambient) (Table 2). Several samples had EC concentrations greater than the manufacturer-given EC threshold of $25 \mu\text{g}/\text{cm}^2$. The

TABLE 1
Temperature protocols for the 3 methods

Step	Atm.	NIST-EPA			NIOSH			IMPROVE		
		Temp. (°C)	RT (s)	Ramp Rate (°C/s)	Temp. (°C)	RT (s)	Ramp Rate (°C/s)	Temp. (°C)	Est. RT (s)*	Avg. Ramp Rate (°C/s)†
OC1	He	200	60	3	310	70	4	120	120	1
OC2	He	400	60	7	475	60	8	250	120	2
OC3	He	600	60	10	615	60	10	450	120	3
OC4	He	785	150	5	870	105	8	550	120	4
Cool	He	550	60	9	550	60	9	550	120	4
EC1	He-Ox	620	60	10	625	60	10	700	120	5
EC2	He-Ox	690	45	15	700	60	12	850	120	6
EC3	He-Ox	760	45	17	775	60	13			
EC4	He-Ox	830	45	18	890	110	8			
EC5	He-Ox	900	90	10						

*RT—residence time at each temperature in the IMPROVE method depend on when the flame ionization detector (FID) signal returned to the baseline.

†Average ramp rate for the IMPROVE protocol is calculated from a residence time of 120 s. To calculate a residence time of 150 s, multiply by 1.25.

percent samples over this threshold for cookstove was 22% (NIOSH TOT), 26% (NIOSH TOR), 24% (IMPROVE TOT), and 37% (IMPROVE TOR). For urban samples, it was 31% (NIOSH TOT), 26% (NIOSH TOR), 53% (IMPROVE TOT), and 42% (IMPROVE TOR). For samples above the threshold, there was concern that the instrumental laser signal inadequately responded to pyrolysis due to baseline saturation or “pegging”. However, visual inspection of the thermograms produced for the urban samples revealed the laser signal responded to EC loads of up to 52 $\mu\text{g}/\text{cm}^2$. Moreover, the average OC/EC ratios calculated with and without those samples exceeding the threshold differed by less than 13% for this source. In contrast, the diesel sample thermograms indicated “pegging” at values below 25 $\mu\text{g}/\text{cm}^2$. In this case, we observed that the absorbance varied with sample load and therefore concluded that “pegging” might not necessarily be the issue. Instead, it is believed that virtually none of the diesel samples exhibited pyrolysis. Roughly, 30% of

the cookstove samples showed “pegging” which was estimated to contribute as much as 25% variability in the overall average OC/EC ratio reported. Finally, none of the rural samples exhibit this behavior; the EC concentration for this sample set was <10 $\mu\text{g}/\text{cm}^2$. More information about each sample type is summarized below:

Residential Cookstove Samples

Forty-six samples were obtained from a study designed by Jetter and Kariher (2009) to measure performance and pollutant emissions from a variety of cookstove/fuel combinations using the Bailis et al. (2004) modified Water Boiling Test (WBT). Aerosols were collected on quartz-fiber filters during the 3 heating phases of this test: (1) C—cold start with water at room temperature with stove operated until water reaches boiling temperature, (2) H—hot start commences immediately after the

TABLE 2
Total carbon measurements for NIST-EPA, NIOSH, and IMPROVE protocols. There was no difference for TC between TOT and TOR for the individual protocols

Method Sample type	Average \pm SD ($\mu\text{g}/\text{cm}^2$)	Range ($\mu\text{g}/\text{cm}^2$)	Method Sample type	Average \pm SD ($\mu\text{g}/\text{cm}^2$)	Range ($\mu\text{g}/\text{cm}^2$)
Cookstove NIST-EPA	35.93 \pm 30.25	4.65–109.78	Rural NIST-EPA	11.00 \pm 6.34	2.90–36.07
Cookstove NIOSH	35.56 \pm 30.04	4.61–106.19	Rural NIOSH	10.86 \pm 6.40	2.93–35.62
Cookstove IMPROVE	36.30 \pm 31.32	3.74–112.87	Rural IMPROVE	10.48 \pm 6.43	2.47–35.46
Diesel NIST-EPA	26.05 \pm 7.70	9.72–43.09	Urban NIST-EPA	79.60 \pm 39.74	32.02–156.37
Diesel NIOSH	26.91 \pm 7.91	12.18–44.41	Urban NIOSH	80.18 \pm 42.07	32.04–163.08
Diesel IMPROVE	26.69 \pm 7.76	10.19–44.27	Urban IMPROVE	82.19 \pm 43.00	32.07–174.25

completion of the cold start phase. The pot is refilled with room temperature water and the stove operated until water reaches boiling temperature, and (3) S—simmer phase begins immediately after the hot start phase with the stove, pot, and water hot. The stove is operated until water temperature is just below boiling point. Samples selected for this study consisted of 10 cookstove/fuel combinations for different WBT phases (Table 3).

Laboratory-Generated Diesel Samples

Forty-six diesel exhaust samples were obtained from a study designed to investigate pulmonary toxicity from the inhalation of diesel exhaust particles (Stevens et al. 2009). Samples were collected from a single-cylinder diesel generator set up outdoors and operated under steady-state conditions with approximately 25–30% full load. A gas chromatography-mass spectrometry (GC/MS) analysis identified *n*-alkanes, organic acids, and polycyclic aromatic hydrocarbons (PAHs) in the diesel PM. The inorganic fraction was analyzed by wavelength dispersive Philips PW2404 X-ray fluorescence (XRF) spectrometer and comprised <5% of the total mass and consisted mostly of S, Cl, Zn, Ca, and Fe.

Rural Ambient Samples

Sixty samples were obtained from a study designed to investigate seasonal biogenic OC changes above an experimental loblolly pine (*Pinus taeda*) forest located at the Blackwood Division of Duke Forest Free Atmosphere Carbon Transfer Scheme (FACTS1) Research Site in Orange County, North Carolina. Samples were collected based upon the EPA OAQPS 1-in-6 day sampling schedule beginning January 2008 and ending January 2009. A URG High Volume 3000DB denuder was used to remove organic vapors and a 92.5 SEPM cyclone separator was placed ahead of the filter to collect PM-2.5. Sampling details are described in Geron (2009). The rural samples consisted primarily of OC from biogenic VOC oxidation and biomass burning.

The EC fraction was attributed to biomass combustion and diesel exhaust from a nearby highway (I-40) and a landfill to the east.

Urban Ambient Samples

Nineteen aerosol samples were obtained from a seasonal study impacted by vehicle and biomass burning emissions in an urban environment. Total suspended particles were collected using a high-volume sampler positioned 20 m above ground on a building at the main campus of Nairobi University, Nairobi, Kenya (1.3°S, 36.8°E) (Ma et al. 2010). In Kenya, biomass is used for cooking and heating. Industrial and domestic wastes that contain carbon are also burned for warmth. GC/MS analysis showed that the aerosol samples contained C-12 to C-35 *n*-alkanes and PAH species typical of major world cities. These samples also contained high mineral dust content due to the super coarse diameter cut-off of the sampler.

RESULTS AND DISCUSSION

OC/EC Split Observations

The OC/EC split point was compared between the NIST-EPA TOT and NIOSH TOT methods. For a given sample, many showed similar placement of the OC/EC split point. However, for a few samples the OC/EC split was in the He phase for 1 method and in the He-Ox phase for another method. For the rural samples, 43 of the 60 samples tested showed the split point at the higher He-Ox temperature step—900°C (NIST-EPA) (Figure S1a, shown in the online supplemental information) and 890°C (NIOSH) (Figure S1b, shown in the online supplemental information). For these samples, instrumentally calculated PyC concentrations were higher than EC concentrations, and we observed EC-PyC mass evolving over a short period within the He-Ox phase without a change in laser transmission. The other seventeen rural samples showed all the EC-PyC removal in the latter stage of the He phase—785°C (NIST-EPA) (Figure S1c, shown in the online supplemental information) and 870°C (NIOSH) (Figure S1d, shown in the online supplemental information). For these samples, the laser signal indicated pyrolysis but the instrument recorded no PyC; EC concentrations were also very low (typically <1 $\mu\text{g}/\text{cm}^2$), and carbon evolution occurred primarily in the He phase. Early oxidation in the He phase may be due to the presence of inorganic materials, such as metal oxides (Chow et al. 2001) or sulfates (Huffman 1996), which are able to act as oxidizing agents at high temperatures. The samples represented in the online supplemental information, Figures S1a and b were collected from January 1, 2008 to September 21, 2008 and Figures S1c and d from September 27, 2008 to January 1, 2009. To rule out instrumental changes over time, several of the samples before and after September 27 were re-run 9 months later and the results remained unchanged. Changes in the chemical composition due to seasonal effects may be a contributing factor for the different thermal behavior of samples after September 27. However, further chemical testing will be needed to substantiate this factor.

TABLE 3
Cookstove/fuel/phase combinations

No	Cookstove	Fuel	WBT phase*
1	Open fire (3-stone)	Kiln-dried Douglas fir	S
2	GTZ	Charcoal	H S
3	Philips	Kiln-dried Douglas fir	C H S
4	Philips	Seasoned oak	C H S
5	UCODEA rocket	Seasoned oak	C H S
6	UCODEA rocket	Charcoal	H S
7	VITA	Kiln-dried Douglas fir	C S
8	VITA	Seasoned oak	S
9	WFP rocket	Kiln-dried Douglas fir	C H S
10	WFP rocket	Seasoned oak	C H S

*C—cold, H—hot, S—simmer (Bailis et al. 2004)

Twelve of the 19 urban samples also showed signs of early light-absorbing carbon (LAC) evolution toward the end of the He phase [Figures S2a (NIST-EPA) and b (NIOSH), shown in the online supplemental information]. Mineral oxides (e.g., iron oxide) from the dust present in the urban samples may have facilitated this premature oxidation. The other 7 urban samples showed EC evolution in the He-Ox phase (Figures S2c [NIST-EPA] and d [NIOSH], shown in the online supplemental information). These urban samples showed little to no PyC, possibly due to a diesel component which contains nonpyrolyzing organic matter, such as PAHs. All the diesel samples showed no PyC and their thermograms mirrored the urban sample thermograms in Figures S2c and d, shown in the online supplemental information. As discussed, no pyrolysis was observed for all diesel samples except for those with $<1 \mu\text{g}/\text{cm}^2$.

Figures S3a (NIST-EPA) and b (NIOSH), displayed in the online supplemental information, show typical thermograms for the cookstove samples. Like the rural and urban samples, there appeared to be some early oxidation in the He phase. For very few samples, the split point was in the He-Ox phase for NIST-EPA and the He phase for NIOSH for the same sample (Figures S3c and d, displayed in the online supplemental information). This discrepancy may be due to “pegging” of the laser signal, which may randomly rise while drifting or with noise, resulting in an erroneous split point. A similar trend was also observed for some of the diesel samples—in some cases the split point was around the third temperature step of the He phase of analysis for the NIST-EPA (Figure S4c, shown in the online supplemental information), while the corresponding NIOSH run was at the end of the He phase (Figure S4d, shown in the online supplemental information). Occasionally a reversal of the split was also observed for NIST-EPA (Figure S4a, shown in the online supplemental information) and the corresponding NIOSH run (Figure S4b, shown in the online supplemental information). [So, noise and drift can be an issue for samples that undergo “pegging” or for those samples that do not pyrolyze (e.g., diesel)]. In general, most of the diesel thermograms looked like Figures S4a for NIST-EPA and d (shown in the online supplemental information) for the corresponding NIOSH run. The unusually large step 4 peak in the He phase coupled with an increase in the laser signal for many of the sample types (urban, cookstove, and diesel) show early carbon oxidization, possibly due to metal catalysis.

Total Carbon (TC)

TC was virtually identical for both transmission and reflectance for all methods. The average and range of TC values for all sample types are shown in Table 2. All 3 protocols (NIST-EPA, NIOSH, and IMPROVE) showed relatively good agreement for each sample type. The r^2 ranged between 0.95 and 0.99 and the slope between 0.97 and 1.04 when NIST-EPA TC was compared with NIOSH TC and IMPROVE TC (Figure S5, displayed in the online supplemental information). Analysis of variance between the methods for each sample type showed no significant differences for TC ($\alpha = 0.05$). A recursive residual

approach was deployed where effects of removal of individual TC values on ANOVA statistics was analyzed. This did not reveal an outlier effect which changed statistical results. Graphical analysis also did not show major outlier effects, and log transformation of TC likewise did not reveal method effects on TC. The low variability between TC values for the 3 methods for the different sample types suggests uniform sample deposits and the overall higher NIST-EPA (900°C) and NIOSH (890°C) temperatures did not release additional carbon beyond the highest IMPROVE temperature (850°C) (Table 1).

Optical and Thermal Effects on Carbon Ratios

The average and range of OC/EC ratios for the different ambient and source-dominated samples are given in Table 4 with emphasis on the optical differences between TOT and TOR. By convention, NIST-EPA and NIOSH are TOT methods and IMPROVE a TOR method. Comparison among the 3 conventional methods shows higher average OC/EC ratios for the TOT methods (Table 4)—with NIST-EPA (TOT) greater than IMPROVE (TOR) by 1.82 (cookstove), 2.01 (diesel), 2.73 (rural), and 1.35 (urban) and NIOSH (TOT) greater than IMPROVE (TOR) by 1.06 (cookstove), 2.73 (rural), 1.97 (diesel), and 1.42 (urban). The optical measurement is critical to distinguishing OC and EC. A TOT/TOR ratio of 1.0 indicates no difference between the optical measures for a particular sample type. Not considering temperature differences, the TOT/TOR OC/EC ratios (Table 4) for each method were highest for the rural and cookstove samples—which also showed higher average PyC/OC ratios (Table S1, shown in the online supplemental information). Diesel and urban TOT/TOR OC/EC ratios were closer to 1.0. Urban samples had the lowest average PyC, and diesel aerosol showed little to no PyC. Although the average OC/EC ratios between NIST-EPA and NIOSH were similar for most of the samples tested; there were cases, particularly among the diesel and rural samples, where NIST-EPA (TOT) values were notably higher than the NIOSH (TOT) causing a wider range of values for the NIST-EPA (TOT). Reasons for the higher NIST-EPA to NIOSH TOT values are due to discrepancies in the position of the split point as mentioned earlier. However, in general, irrespective of TOT or TOR measurements, IMPROVE OC/EC ratios were always slightly lower than NIST-EPA and NIOSH. The optical correction of pyrolysis ascribed to organic vapors can be a factor for describing inconsistencies between TOT and TOR methods (Chow et al. 2004) for the cookstove, diesel, and urban samples. It may be less applicable for the rural samples which were collected using a denuder to filter the organic vapors. For the rural samples, the higher TOT/TOR ratio (compared with the other sample types) may be attributed to volatilization of aerosol particles that passed through the denuder, subsequently adsorbing onto or “in” the filter. Of all the samples tested, the rural samples contained the lowest carbon loading (Table 2) which should magnify any effect due to positive artifact. Another possibility is that liquid-like

TABLE 4

The percent range and average OC/EC ratios for the 3 temperature protocols using optical transmission (TOT) and reflectance (TOR) for char correction. The optical (p value) t -test statistic compares between TOT and TOR for each protocol for each sample type. The thermal (p value) ANOVA-test statistic compares the different temperature protocols within an optical correction method (transmission or reflection). The p values $<.05$ are significantly different (shown in bold).

Method	TOT		TOR		Avg. TOT/TOR	Optical (p value)
	Average \pm SD	Range	Average \pm SD	Range		
Cookstove NIST-EPA	2.29 \pm 2.68	0.28–12.80	1.34 \pm 1.15	0.29–5.39	1.71	.1512
Cookstove NIOSH	2.59 \pm 3.20	0.24–15.33	1.86 \pm 2.00	0.19–9.13	1.39	.1143
Cookstove IMPROVE	1.73 \pm 2.17	0.24–11.62	1.26 \pm 1.43	0.23–6.67	1.37	.0346
Thermal (p value)	.7772		.2696			
Diesel NIST-EPA	2.16 \pm 3.87	0.24–22.58	2.06 \pm 3.91	0.13–22.58	1.05	.3165
Diesel NIOSH	1.54 \pm 2.12	0.27–12.79	1.44 \pm 2.16	0.17–12.78	1.07	.3024
Diesel IMPROVE	0.46 \pm 0.22	0.10–0.97	0.37 \pm 0.25	0.12–0.99	1.24	.0091
Thermal (p value)	.0001		.0001			
Rural NIST-EPA	17.68 \pm 12.86	2.61–84.43	10.83 \pm 21.41	1.63–31.04	1.63	.0001
Rural NIOSH	17.67 \pm 10.09	3.48–58.16	7.92 \pm 4.85	3.88–31.03	2.23	.0001
Rural IMPROVE	13.97 \pm 6.21	1.70–25.71	6.48 \pm 3.80	1.17–21.70	2.16	.0001
Thermal (p value)	.2230		.2460			
Urban NIST-EPA	2.85 \pm 0.77	1.41–4.47	2.54 \pm 0.74	1.27–4.40	1.12	.2010
Urban NIOSH	2.99 \pm 0.76	1.84–5.25	2.79 \pm 0.90	1.46–4.75	1.07	.3307
Urban IMPROVE	1.69 \pm 0.42	1.05–2.60	2.11 \pm 0.65	1.18–3.57	0.80	.0175
Thermal (p value)	.0001		.0293			

particles penetrated the filter to the point where each of the optical measurements interrogated the sample differently.

A plot of the NIOSH TOT-to-NIOSH TOR ratio for the OC/EC split versus total carbon shows that for many of the diesel samples, the ratio was 1.0 (Figure S6, shown in the on-line supplemental information), as expected in the absence of PyC. However, there were inconsistencies between IMPROVE and NIOSH values for the diesel samples. OC concentrations were compared between NIOSH TOT (at 550°C) and IMPROVE TOT (at 550°C). Of the 46 diesel samples, 32 had a NIOSH TOT (870°C)/IMPROVE TOT (500°C) ratio greater than 1.4. Figure S7 in the online supplemental information shows that by comparing NIOSH TOT (550°C) to IMPROVE TOT (550°C) for the samples having a ratio greater than 1.4, NIOSH values were closer to IMPROVE at the same temperature. A similar analysis between NIOSH TOT (550°C) and IMPROVE TOR (550°C) for a ratio greater than 1.5 also showed better OC correspondence for 33 of the 46 diesel samples. For these diesel samples, the better correlation at 550°C (between NIOSH and IMPROVE) suggest that in the absence of PyC the lower temperature protocol may be applicable.

The average and range of EC/TC ratios for the different sample types using the different methods are summarized in Table 5 (and graphically displayed in Figure S8 in the online supplemental information). Results from a 2-tailed t -test are also displayed in Table 5. The test was applied following a

logistic transformation of the EC/TC values to normalize the distribution of data bounded between 0 and 1. The thermal effects on the EC/TC ratio show that for the TOT protocols, cookstove and rural samples were not significantly different ($p > .05$). However, for the diesel and urban samples there were significant differences between the methods ($p < .05$). The TOT protocol driving this difference was the IMPROVE protocol for both the diesel and urban samples. Similar findings were observed for the TOR protocols. An optical comparison between TOT and TOR for the different protocols within a particular sample type shows that cookstove NIST-EPA, diesel IMPROVE, urban IMPROVE, and all of the rural protocols shows some degree of difference because of the optical means of detection. EC/TC for the TOR protocols was generally higher than for the TOT protocols. Analysis of raw, untransformed values of EC/TC yielded similar results.

From a global climate modeling perspective, the large EC/TC range for the cookstove samples (0 to 0.83) is interesting. Cookstove samples tested in this study encompassed 23 cookstove/fuel/WBT phase combinations (Table 3). Figure 2 provides a visual snapshot of the EC/TC ratios for these 23 combinations using the conventional methods (NIST TOT, NIOSH TOT, and IMPROVE TOR). Generally, IMPROVE TOR EC/TC ratios were somewhat higher than for NIST-EPA TOT and NIOSH TOT. WFP rocket stoves gave off the highest overall EC/TC and, oddly enough, EC/TC ratios were low or not

TABLE 5

The percent range and average EC/TC ratios for the 3 temperature protocols using optical transmission (TOT) and reflectance (TOR) for char correction. The optical (p value) t -test statistic compares between TOT and TOR for each protocol for each sample type. The thermal (p value) ANOVA-test statistic compares the different temperature protocols within an optical correction method (transmission or reflection). The p values $<.05$ are significantly different (shown in bold)

Method	TOT		TOR		Optical (p value)
	Average \pm SD	Range	Average \pm SD	Range	
Cookstove NIST-EPA	0.34 \pm 0.23	0.00–0.78	0.43 \pm 0.21	0.00–0.78	.0391
Cookstove NIOSH	0.34 \pm 0.24	0.00–0.78	0.41 \pm 0.21	0.00–0.75	.1724
Cookstove IMPROVE	0.39 \pm 0.24	0.00–0.80	0.50 \pm 0.21	0.00–0.83	.0690
Thermal (p value)	.2583		.293		
Diesel NIST-EPA	0.48 \pm 0.20	0.04–0.80	0.52 \pm 0.24	0.04–0.88	.3165
Diesel NIOSH	0.51 \pm 0.18	0.07–0.79	0.55 \pm 0.21	0.07–0.85	.3024
Diesel IMPROVE	0.70 \pm 0.09	0.51–0.91	0.75 \pm 0.11	0.50–0.89	.0091
Thermal (p value)	.0001		.0001		
Rural NIST-EPA	0.07 \pm 0.04	0.00–0.28	0.14 \pm 0.06	0.01–0.38	.0001
Rural NIOSH	0.07 \pm 0.03	0.02–0.12	0.13 \pm 0.05	0.00–0.24	.0001
Rural IMPROVE	0.08 \pm 0.05	0.00–0.37	0.16 \pm 0.07	0.00–0.46	.0001
Thermal (p value)	.0637		.0587		
Urban NIST-EPA	0.27 \pm 0.06	0.28–0.49	0.29 \pm 0.06	0.21–0.46	.2010
Urban NIOSH	0.26 \pm 0.04	0.18–0.42	0.28 \pm 0.07	0.19–0.44	.3307
Urban IMPROVE	0.38 \pm 0.06	0.16–0.35	0.33 \pm 0.06	0.17–0.41	.0175
Thermal (p value)	.0001		.0293		

detected when charcoal was used as the fuel. However, results from a more comprehensive cookstove study currently being conducted are forthcoming. This study includes 21 cookstoves tested using 6 fuel types under high and low moisture conditions for each WBT phase. Over 200 cookstove/fuel/WBT phase combination samples in triplicate will be collected and analyzed from this study.

“Instrumentally Calculated” Pyrolyzed Carbon (PyC)

A major drawback of the TOA analysis is the susceptibility of certain carbon compounds to char via pyrolysis. Pyrolysis

is a form of incineration that chemically decomposes organic materials by heat in the absence of oxygen. Inaccurate assignment of charred OC results in inaccurate OC/EC ratios. In this paper, PyC measurements were based on the “instrumentally calculated” PyC. It is important to point out that when the laser transmission or reflectance detector is baseline saturated, neither the “instrumentally calculated” PyC nor the “degree of change in the transmission or reflectance response” may be an accurate assessment of how much OC charred. Hence, use of “instrumentally calculated” PyC is only a semi-quantitative indication of charring. For each protocol, the method for

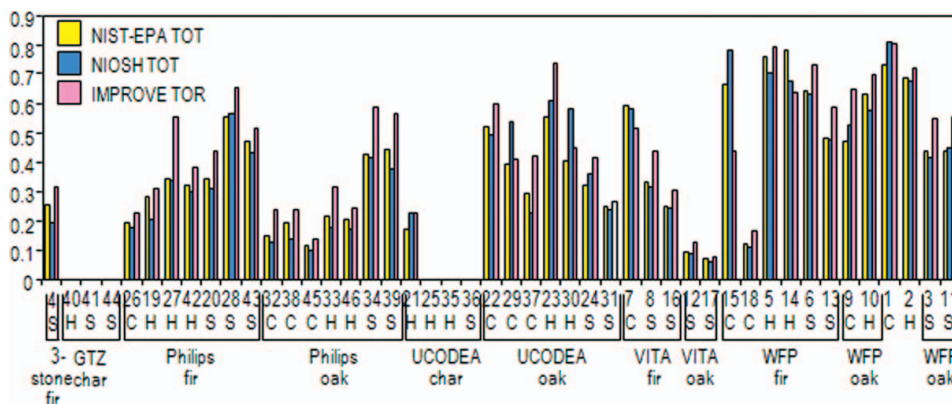


FIG. 2. EC/TC ratios for the different cookstove/fuel/WBT combinations for the conventional methods (NIST-TOT, NIOSH TOT, and IMPROVE TOR) (color figure available online).

determining “instrumentally calculated” PyC was identical, making comparisons between protocols possible. Table S1 (displayed in the online supplemental information) shows the average and range of the “instrumentally calculated” PyC/OC ratio for the different methods within each sample type. All sample types, except for the diesel samples, showed appreciable charring. For the diesel samples, when PyC evolution occurred, it originated in the He phase and values were overall very low, mostly below the instrument’s detection limit ($0.2 \mu\text{g}/\text{cm}^2$). Seventeen of the 60 rural samples also showed early PyC evolution in the He phase (Figure S1c and d, displayed in the online supplemental information). All other samples showed PyC evolution beginning in the He-Ox phase.

For rural, urban, and cookstove samples showing PyC values, IMPROVE PyC values were highest among the 3 protocols, irrespective of whether optical correction was TOT or TOR, suggesting that the pyrolytic behavior of the samples is sensitive to the IMPROVE temperature protocol (Table S1, displayed in the online supplemental information). The heating rates in the He phase for NIOSH and NIST-EPA ranged between 3 and $10^\circ\text{C}/\text{s}$ and was less than $4^\circ\text{C}/\text{s}$ for IMPROVE (if the residence time was 120 or 150 s) (Table 1). The residence time can directly affect the extent of charring, (i.e., the shorter the residence time, the less time for which the sample is subjected to the charring temperatures). Hence, charring may not be complete if the residence time is too short. The higher residence times of the IMPROVE methods may account for the higher PyC. Increasing OC loading also increased PyC for the rural, urban, and cookstove aerosol samples (Figure S6, displayed in the online supplemental information). While the rural and urban samples for the conventional methods showed higher PyC values for IMPROVE TOR than NIOSH TOT, the cookstove values showed little partiality towards either method. Similar results were found between IMPROVE TOR and NIST-EPA TOT. The OC concentrations measured in the cookstove samples were lower than in the rural and urban samples. Of the total carbon, the average %OC values for the rural, urban, and cookstove samples were 84%, 67%, and 50% (IMPROVE TOR); 93%, 72%, and 49% (NIOSH TOT); and 93%, 73%, and 52% (NIST-EPA TOT), respectively.

The aerosol chemical composition can also influence the amount of PyC. Past analysis of these samples showed that the OC composition of the rural samples resulted predominantly from biogenic VOC oxidation (in spring, summer, and fall) and biomass burning (in winter) (Geron 2009) and for the urban samples it was a complex mixture of hydrocarbons (Ma et al. 2010). The chemical composition of the cookstove samples used in the current study was unavailable. However, biomass smoke is a source of “brown” carbon—a polymeric carbonaceous material that is derived from phenolic and sugar derivatives (Sannigrahi et al. 2006). Brown carbon is water soluble and its absorbance increases strongly from long to short wavelengths (Mayol-Bracero et al. 2002). Brown carbon is also a source of aged biogenic secondary organic compounds in rural

aerosols (Lindberg et al. 1993; Hecobian et al. 2010). Water-soluble organic carbons (WSOCs), such as “brown” carbon and humic-like substances (HULIS), are light absorbing organics that make up 10 to 70% of aerosol OC mass in the southeast U.S. and char easily during TOA (Andreae and Crutzen 1997; Yamasoe et al. 2000; Yang and Yu 2002; Shauer et al. 2003). The presence of “brown” carbon may explain the higher PyC for the rural and cookstove samples (Table S1) and differences between TOT/TOR ratios. Other OC compounds, such as those found in diesel and urban aerosols appear less amenable to charring. For example, PAHs and their methylated, nitrated, and oxygenated derivatives typical of motor vehicular exhaust and motor oil are insoluble in water and do not pyrolyze much (Chow et al. 2001; Schauer et al. 2003; Ono-Ogasawara and Smith 2004).

Overall, the %PyC for the urban samples, which contained components of diesel, biomass burning, and mineral oxides, agreed reasonably well for each TOT method and the corresponding TOR method (Table S1, displayed in the online supplemental information). However, the IMPROVE PyC values were substantially higher for the urban samples than the other sample types—showing the susceptibility of the IMPROVE temperatures to charring. For the cookstove samples, the average %PyC for the NIST-EPA (TOT) and NIOSH (TOT) was 2.3 and 1.6 times greater than NIST-EPA (TOR) and NIOSH (TOR), respectively. The lower TOR PyC averages for the cookstove were due to the fact that 78% (NIST-EPA TOR) compared with 26% (NIST-EPA TOT) and 67% (NIOSH TOR) compared with 43% (NIOSH TOT) of the samples measured $<15\%$ PyC. In addition, many of the NIST-EPA TOR cookstove values measuring 0 to 5% PyC measured substantially higher PyC under NIST-EPA TOT (11 and 38%) illustrating how optical effects can influence the measurements. Overall, TOT values for the rural and cookstove samples were higher than the corresponding TOR values. The overall higher TOT values may be attributed to the laser technique, in that TOT penetrates and records PyC deposits throughout the filter material, whereas TOR measures deposits on only the filter surface.

CONCLUSION

Three thermal-optical protocols run on a Sunset Laboratory Dual Optics (transmission and reflectance) Carbon Analyzer was used to measure the OC/EC and EC/TC ratios in several aerosol types. The 3 temperature protocols were: (1) two modified versions of the Birch and Cary (1996) NIOSH 5040 protocol (designated in this paper as NIOSH and NIST-EPA) and (2) the IMPROVE protocol used by the DRI IMPROVE network (designated in this paper as IMPROVE). It should be noted that the DRI network currently uses IMPROVE-A, which is a modified version of the IMPROVE protocol to accommodate for an instrumentation upgrade. Each protocol was run utilizing simultaneous optical transmission (TOT) and optical reflectance (TOR) for char correction. Intercomparison analysis was

conducted among the methods to show the extent to which temperature and optics influenced OC/EC and EC/TC ratios for aerosol emissions from residential cookstoves, urban aerosol collected in Nairobi, Kenya, diesel exhaust, and a rural North Carolina forest.

Results highlight why a single thermal-optical protocol to measure carbon speciation may not be feasible for all sample types. Differences in sample chemical composition, sample behavior under different thermal conditions, optical technique, and sampling technique (specifically, carbon loading) add to the complexity of the measurement. High EC loading can mask the occurrence of charring and cause “pegging” of the laser signal that may result in an inaccurate OC/EC split point. The diesel samples examined for the present study showed no appreciable charring, but may have been susceptible to a similar effect due to laser signal drift and noise.

Comparison between the 3 TOT protocols (NIST-EPA, NIOSH, and IMPROVE) for average OC/EC showed that IMPROVE TOT was typically lower than the other 2 TOT protocols. Similar findings were observed between the TOR methods. These differences illustrate the extent to which temperature influences the OC/EC ratio. Further comparison showed an additional reduction in the average OC/EC ratios for IMPROVE TOR when compared with IMPROVE TOT. This additional reduction is attributed to the optical effects on the measurements. A similar analysis on the EC/TC ratios showed that IMPROVE TOT was higher than the other 2 TOT protocols, with an additional increase (except for the urban samples which showed a decrease) due to optics between IMPROVE TOT and IMPROVE TOR.

OC/EC TOT and the corresponding TOR ratios showed better correlation for the diesel-impacted urban and diesel aerosols but not for the rural and cookstove aerosols. This TOT/TOR discrepancy can be attributed to lack of charring for diesel and diesel-impacted samples, which may contain water insoluble OC that does not easily char during TOA. Rural and biomass emissions contain sizeable fractions of water soluble OC that char during TOA. Differences between laser techniques (TOT and TOR) are have been documented.

On the basis of the overall study findings, no one thermal-optical protocol for measuring carbon ratios can be considered applicable for all types of aerosols samples. Additional research is needed to better understand what happens to a sample during charring, which compounds char, and better optical characterization between charred OC and native EC for the different aerosol types. In TOA, the sample chemical composition plays an important role in char production, which in turn is an integral step to OC/EC determination. However, as observed in the diesel aerosol, in the absence of charring, thermal and optical effects can still be observed, especially for the IMPROVE TOR method. Nonetheless, without some type of standard for OC and EC in atmospheric particulate matter there will always be some level of uncertainty in the data.

REFERENCES

- Andreae, M. O., and Crutzen, P. J. (1997). Atmospheric aerosols: Biogeochemical Sources and Role in Atmospheric Chemistry. *Science*, 276:1052–1058.
- Bailis, R., Ogle, D., Still, D., Smith, K. R., and Edwards, R. (2004). *The Water Boiling Test (WBT), Version 1.5*. University of California, Berkeley, Berkeley, California.
- Birch, M. E. (1998). Analysis of Carbonaceous Aerosols: Inter-laboratory Comparison. *Analyst*, 123:851–857.
- Birch, M. E., and Cary, R. A. (1996). Elemental Carbon-Based Method for Monitoring Occupational Exposures to Particulate Diesel Exhaust. *Aerosol Sci. Technol.*, 25:221–241.
- Bond, T. C., Streets, D. G., Yarber, K. F., Nelson, S. M., Woo, J.-H., and Klimont, Z. (2004). A Technology-Based Global Inventory of Black and Organic Carbon Emissions from Combustion. *J. Geophys. Res.*, 109(014203):43.
- Cavalli, F., Viana, M., Yttri, K. E., Genberg, J., and Putaud, J.-P. (2010). Toward a Standardised Thermal-Optical Protocol for Measuring Atmospheric Organic and Elemental Carbon: The EUSAAR Protocol. *Atmos. Meas. Technol.*, 3:79–89.
- Chow, J. C., Watson, J. G., Chen, L. W., Arnott, W. P., Moosmüller, H., and Fung, K. (2004). Equivalence of elemental carbon by thermal/optical reflectance and transmittance with different temperature protocols. *Environ. Sci. Technol.*, 38(16):4414–4422.
- Chow, J. C., Watson, J. G., Crow, D., Lowenthal, D. H., and Merrifield, T. (2001). Comparison of IMPROVE and NIOSH Carbon Measurements. *Aerosol Sci. Technol.*, 34(1):23–34.
- Chow, J. C., Watson, J. G., Pritchett, L. C., Pierson, W. R., Frazier, C. A., and Purcell, R. G. (1993). The DRI Thermal/Optical Reflectance Carbon Analysis System: Description, Evaluation, and Applications in U.S. Air Quality Studies. *Atmos. Environ.*, 27:1185–1201.
- Conny, J. (2007). *The Optimization of Thermal-Optical Analysis for the Measurement of Black Carbon in Regional PM2.5: A Chemometric Approach*. U.S. Report EPA 600/R-07/119. Environmental Protection Agency, Office of Research and Development, Washington, DC.
- Countess, R. J. (1990). Inter-laboratory Analyses of Carbonaceous Aerosol Samples. *Aerosol Sci. Technol.*, 12(1):114–121.
- Crutzen, P. J., and Ramanathan, V. (2003). Atmospheric Chemistry and Climate in the Anthropocene: Where Are We Heading? in *Earth System Analysis for Sustainability*, H. J. Schellnhuber, P. J. Crutzen, W. C. Clark, M. Claussen, and H. Held, eds. MIT Press, Cambridge, MA, pp. 265–292.
- Geron, C. (2009). Carbonaceous Aerosol Over a *Pinus taeda* Forest in Central North Carolina, USA. *Atmos. Environ.*, 43:959–969.
- Hansen, J., Sato, M., Ruedy, R., Lacis, A., and Oinas, V. (2000). Global Warming in the Twenty-First Century: An Alternative Scenario. *Proc. Nat. Acad. Sci.*, 97:9875–9880.
- Hecobian, X., Zhang, M., Zheng, N., Frank, E., Edgerton, S., and Weber, R. J. (2010). Brown Carbon and Water-soluble Organic Aerosols over the Southeastern United States. *Atmos. Chem. Phys. Discuss.*, 10:7601–7639.
- Huffman, H. D. (1996). Comparison of the Light Absorption Coefficient and Carbon Measures for Remote Aerosols: An Independent Analysis of Data from the IMPROVE Network – I. *Atmos. Environ.*, 30:73–83.
- IPCC (2007). *Climate Change 2007: The physical science basis. Summary for policymakers*. Contribution of Working Group I to the Fourth Assessment Report of the Intergovernmental Panel on Climate Change, Intergovernmental Panel on Climate Change (IPCC), Geneva, Switzerland.
- Jacobson, M. Z. (2001). Strong Radiative Heating Due to the Mixing State of Black Carbon in Atmospheric Aerosols. *Nature*, 409:695–697.
- Jetter, J. J., and Kariher, P. (2009). Solid Fuel Household Cook Stoves: Characterization of Performance and Emissions. *Biomass Bioenerg.*, 33:294–305.
- Kagawa, J. (2002). Health Effects of Diesel Exhaust Emissions - A Mixture of Air Pollutants of Worldwide Concern. *Toxicology*, 181–182:349–353.
- Lindberg, J. D., Douglass, R. E., and Garvey, D. M. (1993). Carbon and the Optical Properties of Atmospheric Dust. *Appl. Opt.*, 32:6077–6081.

- Ma, Y., Hays, M. D., Geron, C. D., Walker, J. T., and Gatari Gichuru, M. J. (2010). Technical Note: Fast two-Dimensional GC-MS with Thermal Extraction for Anhydro-Sugars in Fine Aerosols. *Atmos. Chem. Phys.*, 10:4331–4341.
- Mader, B. T., Flagan, R. C., and Seinfeld, J. H. (2001). Sampling Atmospheric Carbonaceous Aerosols Using a Particle Trap Impactor/Denuder Sampler. *Environ. Sci. Technol.*, 35(24):4857–4867.
- Mayol-Bracero, O. L., Guyon, P., Graham, B., Roberts, G., Andreae, M. O., Decesari, S., et al. (2002). Water-soluble Organic Compounds in Biomass Burning Aerosols over Amazonia 2. Apportionment of the Chemical Composition and Importance of the Polyacidic Fraction. *J. Geophys. Res.*, 107:8091, 15.
- Ono-Ogasawara, M., and Smith, T. J. (2004). Diesel Exhaust Particles in the Work Environment and their Analysis. *Ind. Health*, 42:389–399.
- Pope, C. A. III, and Dockery, D. W. (2006). Health Effects of Fine Particulate Air Pollution: Lines That Connect. *J. Air Waste Manag. Assoc.*, 56(6):709–742.
- Sannigrahi, P., Sullivan, A. P., Weber, R. J., and Ingall, E. D. (2006). Characterization of Water-Soluble Organic Carbon in Urban Atmospheric Aerosols Using ¹³C NMR Spectroscopy. *Environ. Sci. Technol.*, 40:666–672.
- Schmid, H., Laskus, L., Abraham, H. J., Baltensperger, U., Lavanchy, V., Bizjak, M., et al. (2001). Results of the “Carbon Conference” International Aerosol Carbon Round Robin Test Stage I. *Atmos. Environ.*, 35:2111–2121.
- Schauer, J. J., Mader, B. T., DeMinter, J. T., Heidemann, G., Bae, M. S., Seinfeld, J. H., et al. (2003). ACE-Asia Intercomparison of a Thermal-Optical Method for the Determination of Particle-Phase Organic and Elemental Carbon. *Environ. Sci. Technol.*, 37(5):993–1001.
- Stevens, T., Cho, S.-H., Linak, W. P., and Gilmour, M. I. (2009). Differential Potentiation of Allergic Lung Disease in Mice Exposed to Chemically Distinct Diesel Samples. *Toxicol. Sci.*, 107(2):522–534.
- Subramanian, R., Khlystov, A. Y., Cabada, J. C., and Robinson, A. L. (2004). Evaluation of Measurement Methods: Positive and Negative Artifacts in Particulate Organic Carbon Measurements with Denuded and Undenuded Sampler Configurations. *Aerosol Sci. Technol.*, 38(S1):27–48.
- Subramanian, R., Khlystov, A. Y., and Robinson, A. L. (2006). Effect of Peak Inert-Mode Temperature on Elemental Carbon Measured Using Thermal-Optical Analysis. *Aerosol Sci. Technol.*, 40(10):763–780.
- Yamasoe, M. A., Artaxo, P., Miguel, A. H., and Allen, A. G. (2000). Chemical Composition of Aerosol Particles from Direct Emissions of Vegetation Fires in the Amazon Basin: Water-soluble Species and Trace Elements. *Atmos. Environ.*, 34:1641–1653.
- Yang, H., and Yu, J. Z. (2002). Uncertainties in Charring Correction in the Analysis of Elemental and Organic Carbon in Atmospheric Particles by Thermal/Optical Methods. *Environ. Sci. Technol.*, 36:5199–5204.
- Yu, J. Z., Xu, J., and Yang, H. (2002). Charring Characteristics of Atmospheric Organic Particulate Matter in Thermal Analysis. *Environ. Sci. Technol.*, 36(4):754–761.
- United States Agency International Development [USAID] (2010). *Black Carbon Emissions in Asia: Sources, Impacts, and Abatement Opportunities*. Contract No. EPP-1–100-03–00013-00: Task Order 9. International Resources Group (IRG).
- Watson, J. G. (2002). Visibility: Science and regulation—2002 Critical Review. *J. Air Waste Manag. Assoc.*, 52:628–713.
- Zhi, G., Chen, Y., Sheng, G., and Fu, J. (2009). Effects of Temperature Parameters on Thermal-Optical Analysis of Organic and Elemental Carbon in Aerosol. *Environ. Monitor. Assess.*, 154(1–4):253–261.